

# Single-shot quantum nondemolition measurement of a quantum-dot electron spin using cavity exciton-polaritons

Shruti Puri,<sup>1,\*</sup> Peter L. McMahon,<sup>1,\*</sup> and Yoshihisa Yamamoto<sup>1,2</sup><sup>1</sup>*E. L. Ginzton Laboratory, Stanford University, Stanford, California 94305, USA*<sup>2</sup>*National Institute of Informatics, 2-1-2 Hitotsubashi, Chiyoda-ku, Tokyo 101-8430, Japan*

(Received 21 October 2013; revised manuscript received 26 September 2014; published 13 October 2014)

We propose a scheme to perform single-shot quantum nondemolition (QND) readout of the spin of an electron trapped in a semiconductor quantum dot (QD). Our proposal relies on the interaction of the QD electron spin with optically excited, quantum well (QW) microcavity exciton-polaritons. The spin-dependent Coulomb exchange interaction between the QD electron and cavity polaritons causes the phase and intensity response of left circularly polarized light to be different than that of right circularly polarized light, in such a way that the QD electron's spin can be inferred from the response to a linearly polarized probe reflected or transmitted from the cavity. We show that with careful device design it is possible to essentially eliminate spin-flip Raman transitions. Thus a QND measurement of the QD electron spin can be performed within a few tens of nanoseconds with fidelity  $\sim 99.95\%$ . This improves upon current optical QD spin readout techniques across multiple metrics, including speed and scalability.

DOI: [10.1103/PhysRevB.90.155421](https://doi.org/10.1103/PhysRevB.90.155421)

PACS number(s): 78.67.Hc, 03.67.Lx, 78.67.De, 78.67.Pt

## I. INTRODUCTION

The ability to measure a single electron spin by projecting it onto the eigenstate corresponding to the measurement result, constitutes a quantum nondemolition (QND) measurement and is of great importance in measurement-based quantum computing schemes [1]. Since the electron spin is projected onto an eigenstate, the measurement can be repeated several times and should give the same result for subsequent measurements. Thus, classical noise can be reduced by time averaging. This method can be used for faithful initialization and measurement of qubits [2].

Any proposed QND spin measurement scheme should use a physical process that is unlikely to cause a spin-flip event for the duration of the measurement. In an optical measurement scheme based on the Faraday rotation induced by a confined spin, the spin-flip Raman scattering must be suppressed [3,4]. One way to overcome this adverse effect is to use a quantum dot (QD) molecule, which has separate optical transitions for state preparation, manipulation, and measurement; spin readout by collection of fluorescence from one of these transitions has been demonstrated [5]. However, even in this system the probe laser has a non-negligible probability of causing the spin to flip ( $\approx 7\%$  in [5]). Furthermore, the measurement is quite slow, taking  $\sim 2$  ms to achieve a fidelity of 96%. Finally, the use of QD molecules in a large-scale quantum computing system has the disadvantage that it is difficult to deterministically grow arrays of spectrally homogeneous QD molecules. Recently, a demonstration of the readout of a QD spin by collecting fluorescence from a pseudocycling transition was reported [6]. The measurement was carried out within 800 ns, but the fidelity was limited to 82%. In this paper, we propose a QND readout scheme for QD electron spins in Faraday geometry, which differs from previous proposals and implementations in that it relies on a novel physical mechanism: the interaction of a

QD spin with optically excited quantum well (QW) exciton-polaritons.

## II. MEASUREMENT SCHEME

### A. System

In Faraday geometry, a QD electron spin is quantized along the growth ( $z$ ) axis, by an external magnetic field  $B_0\hat{z}$ . The system we consider in this paper, illustrated in Fig. 1, consists of an  $\text{In}_x\text{Ga}_{1-x}\text{As}$  QD grown on top of an  $\text{In}_y\text{Ga}_{1-y}\text{As}$  QW. Between them is a few-monolayer-thick GaAs barrier layer. The QD and QW are embedded in a GaAs  $\lambda$  cavity formed by AlGaAs/AlAs distributed Bragg mirrors (DBRs). The QW exciton is resonant with the cavity photons at  $\mathbf{k}_{\parallel} = \mathbf{0}$ . In the strong coupling regime, bare QW excitons and cavity photons coherently exchange energy faster than the rate at which the photons are lost from the cavity. The resulting eigenmodes are upper polaritons (UPs) and lower polaritons (LPs), as depicted in Fig. 2(a) [8]. The splitting between them depends on the strength of the coupling between QW excitons and cavity photons. A red-detuned ( $\delta$ ), left (right) circularly polarized  $\{\sigma^+ (\sigma^-)\}$  laser pulse excites LPs in the region below the QD, as shown in Fig. 1(a). Because of the QW exciton selection rules, LPs with total angular momentum along the growth direction  $J_z = +1(-1)$  and  $\mathbf{k}_{\parallel} = \mathbf{0}$  are excited in the area (A) under the laser spot [9]. The excitonic component of the LP is composed of an electron with  $s_{ze} = -\frac{1}{2}(+\frac{1}{2})$  and a heavy hole with  $l_{zhh} = +1(-1)$ ,  $s_{zhh} = +\frac{1}{2}(-\frac{1}{2})$ , where  $s$  and  $l$  refer to spin and orbital angular momentum [10,11]. Excitons with  $s_{ze} = +\frac{1}{2}(-\frac{1}{2})$ ,  $l_{zhh} = +1(-1)$ , and  $s_{zhh} = +\frac{1}{2}(-\frac{1}{2})$  are optically dark states. If the duration of the laser pulse is much longer than the inverse of optical detunings in the system, then the polaritons evolve adiabatically according to

$$\alpha_{1(-1)}(t) = \frac{\sqrt{\gamma_1} t_0 f(t)_{1(-1)}}{i\delta + \frac{(\gamma_1 + \gamma_2)}{2}}.$$

Here,  $\alpha_{1(-1)}$  are the coherent amplitudes of the LP with  $J_z = 1(-1)$ , and  $|f(t)_{1(-1)}|^2$  are the input photon fluxes in  $\sigma^+$  ( $\sigma^-$ )

\*These authors contributed equally.

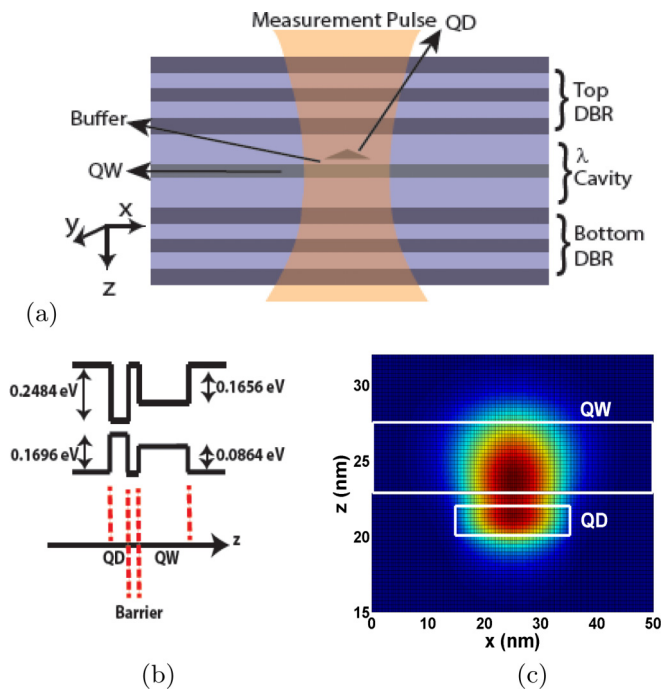


FIG. 1. (Color online) (a) Illustration of the system consisting of a QD grown on a QW placed in a GaAs  $\lambda$  microcavity. An electron is trapped in the QD. A probe laser incident over the QD, excites polaritons in the microcavity. (b) Band structure of the QD and QW system. The effective mass of electron (hole) in  $\text{In}_{0.3}\text{Ga}_{0.7}\text{As}$  is  $0.0504m_0$  ( $0.48m_0$ ) and that in  $\text{In}_{0.15}\text{Ga}_{0.85}\text{As}$  is  $0.0566m_0$  ( $0.495m_0$ ), where  $m_0$  is the mass of a free electron. (c) Numerically evaluated, normalized wave function distribution ( $|\psi(\mathbf{r})|^2$ ) of the QD electron along the  $x$  and  $z$  axes at  $y = 25$  nm (the Schrödinger equation is discretized in a cuboid region of size  $50$  nm  $\times$   $50$  nm  $\times$   $50$  nm). The white rectangles mark the QD and QW regions [7].

polarizations,  $\gamma_1$  ( $\gamma_2$ ) are the polariton decay rates from the top (bottom) DBR mirror, and  $t_0$  is the photon Hopfield factor for LPs [8].

### B. Measurement mechanism: Coulomb exchange interaction

A self-assembled  $\text{In}_x\text{Ga}_{1-x}\text{As}$  QD has a pyramidal shape with a typical height of  $\sim 1.5$  nm and base width of  $\sim 20$  nm. An  $\text{In}_y\text{Ga}_{1-y}\text{As}$  QW can be grown 6 nm thick. By carefully choosing the barrier layer thickness and In concentrations ( $x$  and  $y$ ) one can design the band structure such that the electron confined in the QD has a nonzero wave function in the QW [Figs. 1(b) and 1(c)]. The finite overlap of the localized QD electron and microcavity polariton results in a spin-dependent Coulomb exchange interaction between them [12–14]:

$$H_1 = -V_{\text{ex}} \hat{\sigma}_1 \cdot \hat{\sigma}_e,$$

$$V_{\text{ex}} = |r_0|^2 \int d\mathbf{r}_e d\mathbf{r}_2 d\mathbf{r}_1 \frac{\psi(\mathbf{r}_e, \mathbf{r}_2) \phi(\mathbf{r}_1) e^2 \psi(\mathbf{r}_1, \mathbf{r}_2) \phi(\mathbf{r}_e)}{4\pi\epsilon |\mathbf{r}_e - \mathbf{r}_1|},$$

where  $\epsilon$  is the dielectric constant of the  $\text{In}_y\text{Ga}_{1-y}\text{As}$  QW,  $\mathbf{r}_1, \mathbf{r}_2$  are the position vectors of the electron and hole in the excitonic part of the polariton,  $\mathbf{r}_e$  is that of the QD electron,  $\psi$  and  $\phi$  represent the wave functions of the excitonic component of the polariton and of the localized electron, and  $\hat{\sigma}_e$  ( $\hat{\sigma}_1$ ) are the Pauli spin operators of the QD electron (electronic part of

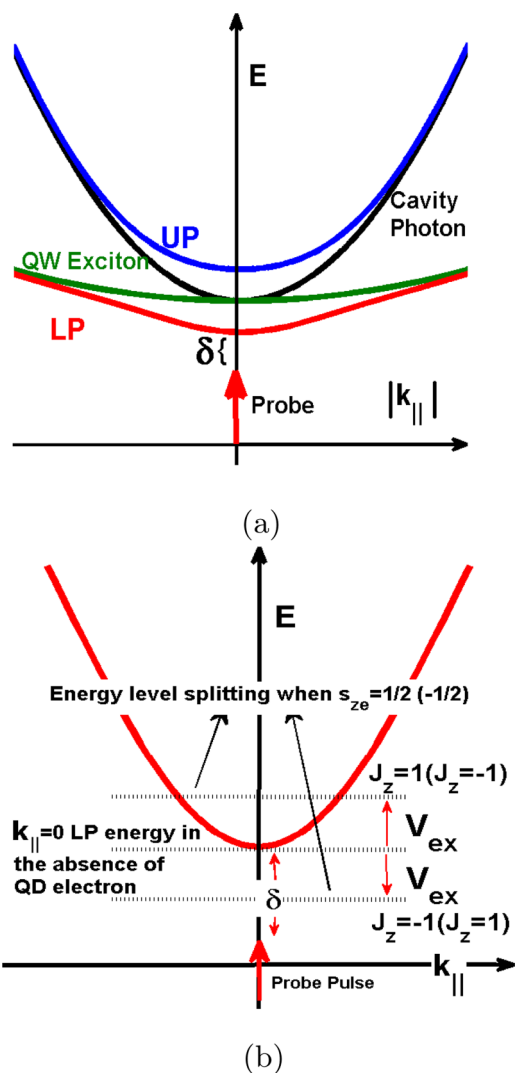


FIG. 2. (Color online) (a) Representation of the exciton polariton energy dispersion. The green (black) line is the bare exciton (cavity photon) dispersion curves and blue (red) solid lines are that for the UPs (LPs). (b) Exaggerated depiction of the energy level splitting of the  $J_z = 1$  and  $J_z = -1$  LP modes. If the QD electron spin  $s_{ze} = \frac{1}{2}$  ( $-\frac{1}{2}$ ), then the energy of the  $J_z = -1$  polariton is red-detuned (blue-detuned) from the  $J_z = 1$  polariton by  $2V_{\text{ex}}$ .

polariton). From here on subscript “1” (“2”) will describe the electronic (hole) component in the polariton and the subscript “e” will describe the electron in the QD.  $r_0$  is the excitonic Hopfield coefficient of  $\mathbf{k}_{\parallel} = \mathbf{0}$  LPs. Since the cavity photons and QW excitons are resonant at  $\mathbf{k}_{\parallel} = \mathbf{0}$ ,  $r_0 = 1/\sqrt{2}$ . We have ignored the exchange interaction between the QD electron and the hole part of the LP. This is because the different Bloch wave functions for the electron ( $s$ -like in conduction band) and the hole ( $p$ -like in valence band) leads to a smaller exchange energy [15]. The unique area ( $A = \pi R^2$ ) in the QW in which single mode ( $\mathbf{k}_{\parallel} = \mathbf{0}$ ) polaritons are coherently excited depends on the cavity lifetime ( $\tau$ ) [7, 16–21]. For example, for the cavity photon lifetime  $\tau = 4$  ps,  $R = 3.6$   $\mu\text{m}$  [7]. If  $x = 30\%$ ,  $y = 15\%$ , the barrier layer is 1 nm thick, and the pump laser excites the LPs in a spot of radius  $R = 3.6$   $\mu\text{m}$ ,

then we estimate that  $V_{\text{ex}} \approx 0.2 \mu\text{eV}$  [7]. We have designed a sample for which the band structure is such that the QD trion resonance (937 nm) is detuned from the QW exciton resonance (918 nm) by  $\sim 27$  meV. This ensures that the probe pulse, which has a frequency near that of the QW exciton resonance, is far detuned from the  $s$ -,  $p$ -, and higher-shell QD trion resonances. This results in a very low probability for the probe pulse to cause a QD spin flip by Raman scattering.

The exchange interaction gives rise to not only spin-conserving but also spin-flip terms. The spin-conserving term induces a spin-dependent shift in the polariton resonance. If  $s_{ze} = +\frac{1}{2}$ , then the resonance energy of a  $J_z = -1$  (+1) LP will decrease (increase) by an amount  $V_{\text{ex}}$ , making the  $J_z = 1$  and  $J_z = -1$  polaritons nondegenerate as shown in Fig. 2(b). (This effect is reversed if  $s_{ze} = -\frac{1}{2}$ .) We will exploit these spin-dependent polariton resonance shifts to measure the spin of the QD electron. If the localized electron undergoes a spin flip, the LP will be scattered as a dark exciton. The dark exciton is blue-detuned by  $\Delta_{\text{dark}} \sim 1$  meV from the LPs at  $\mathbf{k}_{\parallel} = \mathbf{0}$  and thus this scattering is made possible only by phonon absorption. It can be shown that the spin-flip probability in our proposed scheme is negligible [7]. The total Hamiltonian of the system in the frame rotating at the frequency of the probe pulse can be written as

$$H = \delta p_1^\dagger p_1 + \delta p_{-1}^\dagger p_{-1} - V_{\text{ex}} \hat{\sigma}_{ze} p_1^\dagger p_1 + V_{\text{ex}} \hat{\sigma}_{ze} p_{-1}^\dagger p_{-1} + \sqrt{\gamma_1} f_{\text{in}} (p_1^\dagger + p_1) + \sqrt{\gamma_1} f_{-1\text{in}} (p_{-1}^\dagger + p_{-1}), \quad (1)$$

where  $\delta$  is the detuning of the  $J_z = 1$  and  $J_z = -1$  polaritons from the probe pulse in the absence of the exchange interaction [shown in Figs. 2(a) and 2(b)],  $\hat{\sigma}_{ze} = (|\frac{1}{2}\rangle\langle\frac{1}{2}| - |-\frac{1}{2}\rangle\langle-\frac{1}{2}|)$  is the Pauli spin operator ( $|\pm\frac{1}{2}\rangle$  is the spin state of the localized electron),  $p_1^\dagger(p_{-1}^\dagger)$  are the creation operators of  $J_z = 1(-1)$  polaritons, and  $|f_{\text{in}}|^2(|f_{-1\text{in}}|^2)$  is the polariton flux, i.e., the number of polaritons that are pumped into the QW per unit time. From Eq. (1) we see that the exchange-interaction Hamiltonian between the QD electron spin and QW LPs, represented by the third and fourth terms commutes with  $\hat{\sigma}_{ze}$ . Thus it would be possible to use the QW LPs as readout observables to determine the state of the measured observable  $\sigma_{ze}$  without any backaction.

### C. Measurement setup

The setup for the measurement scheme is illustrated in Fig. 3. A horizontally (H) polarized probe laser pulse is incident on the coupled QD-QW microcavity system (through

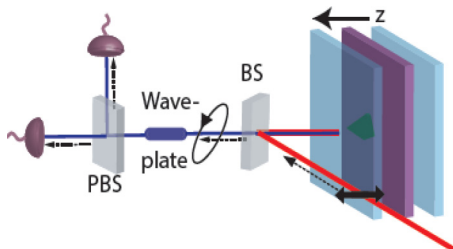


FIG. 3. (Color online) Illustration of the measurement setup.

a 90:10 beam splitter), coherently exciting polaritons with  $J_z = 1$  and  $J_z = -1$ . These polaritons interact with the localized spin and decay from the cavity at rate  $\gamma = \gamma_1 + \gamma_2$ , emitting  $\sigma^+$ - and  $\sigma^-$ -polarized photons, respectively. Because the  $J_z = 1, -1$  polaritons evolve with different frequencies depending on the QD electron spin, the light coupled out from the cavity carries information about the QD spin. As a result, the reflected light is elliptically polarized with its axis tilted by an angle  $\propto \pm V_{\text{ex}}$  (depending on whether  $s_{ze} = \pm\frac{1}{2}$ ). Even in the absence of the QD electron, strain-induced asymmetry during the growth process can lift the degeneracy between H-polarized and vertically (V) polarized polaritons [22,23]. Considering this energy splitting ( $=2V_s$ ), the photon flux reflected from the cavity is

$$\frac{f_{\text{H}}}{f_0} = -1 + \frac{\gamma_1(i\delta_2 + \frac{\gamma}{2})}{V_{\text{ex}}^2 + (i\delta_1 + \frac{\gamma}{2})(i\delta_2 + \frac{\gamma}{2})}, \quad (2)$$

$$\frac{f_{\text{V}}}{f_0} = \frac{\mp\gamma_1 V_{\text{ex}}}{V_{\text{ex}}^2 + (i\delta_1 + \frac{\gamma}{2})(i\delta_2 + \frac{\gamma}{2})}.$$

Here,  $|f_0|^2$  is the H-polarized input photon flux,  $|f_{\text{H}}|^2(|f_{\text{V}}|^2)$  is the reflected photon flux with H (V) polarization, with the  $-$  or  $+$  indicating if  $s_{ze} = +\frac{1}{2}$  or  $-\frac{1}{2}$ .  $\delta_1$  ( $\delta_2$ ) is the detuning of the laser from the H- (V-) polarized LPs in the absence of a QD electron, so that  $\delta_1 - \delta_2 = 2V_s$ . The reflected light from the cavity passes through the 90:10 BS and arrives at the wave plate. The  $\frac{\lambda}{4}$  wave plate, with its axis oriented at  $\frac{\pi}{4}$  (0) rad with respect to the H-V axis rotates the polarization of the field. The polarizing beam splitter, placed at the output of the  $\frac{\lambda}{2}$  ( $\frac{\lambda}{4}$ ) wave plate, oriented along ( $45^\circ$  to) the axis of the wave plates, isolates the two orthogonal polarizations incident on it, which are then measured by detectors  $D_1$  and  $D_2$ . The difference in the photon counts of  $D_1$  and  $D_2$ , when using a  $\frac{\lambda}{2}$  waveplate is

$$I_{D1} - I_{D2} = \left| \frac{f_{\text{H}} + f_{\text{V}}}{\sqrt{2}} \right|^2 - \left| \frac{f_{\text{H}} - f_{\text{V}}}{\sqrt{2}} \right|^2 = 2|f_+||f_-| \sin(\theta_+ - \theta_-), \quad (3)$$

which is the phase response. When using a  $\frac{\lambda}{4}$  wave plate the difference in detector counts is

$$I_{D1} - I_{D2} = \left| \frac{f_{\text{H}} + if_{\text{V}}}{\sqrt{2}} \right|^2 - \left| \frac{f_{\text{H}} - if_{\text{V}}}{\sqrt{2}} \right|^2 = |f_+|^2 - |f_-|^2, \quad (4)$$

which is the intensity response. In the above equations,  $f_+(f_-)$  and  $\theta_+(\theta_-)$  are the amplitudes and phase shifts of the reflected field with  $\sigma^+(\sigma^-)$  polarization [7]. In both cases  $I_{D1} - I_{D2} \propto \pm V_{\text{ex}}$  (for small  $V_{\text{ex}}$ ) if  $s_{ze} = \pm\frac{1}{2}$  and hence can be used to distinguish the spin state of the localized electron spin.

Figure 4 shows the phase and intensity responses in the reflection spectrum of the cavity. If  $s_{z1} = +\frac{1}{2}$ ,  $V_s = 0$ , then  $\delta_1 = \delta_2 = \delta$ . For  $\delta < 0$  ( $\delta > 0$ ), the probe pulse is closer to the  $J_z = -1$  ( $J_z = 1$ ) LP resonance (Fig. 2). As a result, in a two-sided cavity, when  $\delta < 0$  ( $\delta > 0$ )  $\sigma^+$ -polarized light (which excites  $J_z = 1$  LPs) will be reflected more (less) than the  $\sigma^-$  light (which excites  $J_z = -1$  LPs). If  $|\delta| \gg \gamma$ , then neither of the polarization components of the probe pulse are

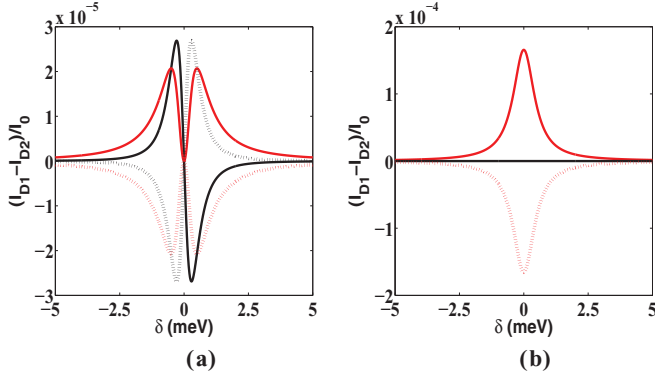


FIG. 4. (Color online) Phase (red) and intensity (black) response when  $V_s = 0$ , (a)  $\gamma_1 = \gamma_2 = 0.5$  meV, (b)  $\gamma_1 = 1$  meV,  $\gamma_2 = 0$ . The solid (dashed) lines represent the response with the QD electron spin  $s_{ze} = \frac{1}{2}$  ( $-\frac{1}{2}$ ).

able to enter the cavity. Consequently, there is no information about the spin state of the QD electron in the reflected light and from Eq. (4),  $I_{D1} - I_{D2} = 0$ . At  $\delta \approx \pm\gamma/(2\sqrt{3})$  the intensity response becomes maximal. These results can be seen in the intensity response shown in Fig. 4(a). On the other hand, in a single-sided cavity, for all values of detuning  $\delta$ , both the  $\sigma^+$  and  $\sigma^-$  light are completely reflected from the cavity. Hence, the intensity response vanishes [Fig. 4(b)]. The phase response from a two-sided cavity can be understood as follows: At  $\delta = V_{ex}(-V_{ex})$ , the probe is resonant with the  $J_z = 1(-1)$  polariton mode. Hence,  $f_+(f_-) = 0$  and from Eq. (3) for the dispersive response,  $I_{D1} - I_{D2} = 0$ . In a two-sided cavity,  $\tan(\theta_+) = \frac{\gamma}{2(\delta + V_{ex})}$  and  $\tan(\theta_-) = \frac{\gamma}{2(\delta - V_{ex})}$ . As shown in Fig. 4(a), the maximum in the phase response appears at  $\delta \approx \pm\gamma/2$ . In a single-sided cavity  $\tan(\theta_+) = 4(\delta + V_{ex})/\gamma$  and  $\tan(\theta_-) = 4(\delta - V_{ex})/\gamma$ . Its phase response is shown in Fig. 4(b). Unlike the two-sided cavity, the phase response of a single-sided cavity is maximal at  $\delta = 0$ . If  $s_{z1} = -\frac{1}{2}$  then the  $J_z = 1$  polariton mode has lower energy than the  $J_z = -1$  mode and the response curves are just reversed [dotted lines in Figs. 4(a) and 4(b)]. Thus a measurement  $I_{D1} - I_{D2}$  will reveal the spin state of the electron. In a real experimental system  $V_s \neq 0$  and we can plot and explain the response curves [7] for a typical H-V nondegeneracy of  $V_s = 0.15$  meV [22,23]. It is important to note that the external magnetic field (typically between 2 and 4 T) applied along the growth axis (or  $z$  axis) to define the qubit also lifts the degeneracy between the  $J_z = 1$  and  $J_z = -1$  excitons [24]. However, this shift is independent of the QD electron spin state. The external magnetic field shrinks the exciton wave function, leading to a change in the exciton oscillator strength. However, this effect is negligible at low magnetic fields. Furthermore, it changes the excitonic fraction ( $|r_0|^2$ ) in the  $J_z = 1$  and  $J_z = -1$  LPs. We analyze these effects of the Faraday magnetic field on the readout signal in the Supplemental Material [7]. We show that, unlike the H-V nondegeneracy, the splitting between the  $J_z = 1$  and  $J_z = -1$  LPs ( $\sim 100$   $\mu$ eV for  $B_0 = 2$  T) leads to a nonzero signal in the absence of the QD electron. This acts as a baseline and can be subtracted from the readout signal to reveal the spin state of the QD electron [7].

### III. MEASUREMENT TIME AND FIDELITY

As explained previously, one source of erroneous operation in this measurement scheme is the phonon-assisted, spin-flip scattering and its probability is  $P_e^{\text{dark}} \sim \Gamma^{\text{dark}} \tau_{\text{meas}}$  where  $\Gamma^{\text{dark}} = 63\,300$  s $^{-1}$  (418 s $^{-1}$ ) at  $T = 1.5$  K for a single-sided (two-sided) cavity [7]. In addition, we optically excite  $N$  exciton-polaritons and the QD electron can radiatively recombine with any of the  $N$  hole states in the QW. We find that [7] the oscillator strength of such a transition is very small, leading to a long radiative lifetime  $\tau_0$  ( $\sim 100$  ms). The probability of error during the measurement time  $\tau_{\text{meas}}$  is  $P_e^{\text{rad}} = 1 - e^{-N\tau_{\text{meas}}/\tau_0}$ . Finally, in a photon counting measurement, there are errors due to quantum fluctuations (shot noise). The number of polaritons at steady state is limited to  $N \sim 2000$ , corresponding to a low density of  $\sim 5 \times 10^9$  cm $^{-2}$ , so that, polariton-polariton scattering can be ignored [7]. The measurement time is set by the amount of time needed to probe the system with sufficiently many photons that the maximal signal (in Fig. 4) can be reliably used to discriminate  $s_{ze} = +\frac{1}{2}$  and  $s_{ze} = -\frac{1}{2}$ . Table I shows the measurement times required to make measurements that have a discrimination error of  $P_e^{\text{sn}} = 4 \times 10^{-4}$  due to shot noise [7]. The shot noise error is especially important in a single-shot readout scheme, as only one application of the probe beam should determine the correct state of the qubit with high fidelity. One can measure the spin state of the electron spin qubit within 28 ns (for  $V_s = 0$ ) or 17 ns (for  $V_s = 0.15$  meV), with overall fidelities of  $\sim 99.95\%$ . A single-shot measurement taking only  $\tau_{\text{meas}} \sim 10$  ns, and with a fidelity of 99.95%, would represent a tenfold improvement in speed and large improvement in fidelity over the current best single-shot readout (800 ns, 82% fidelity) [6]. Our proposed scheme should also yield a QND measurement, whereas current single-shot readout demonstrations exhibit substantial spin-flip backaction [5,6]. In optical semiconductor QDs the major source of electron spin decoherence is the hyperfine coupling with nuclear spins. The longitudinal relaxation time ( $T_1$ ) in a singly charged QD is of the order of tens of milliseconds, for an external magnetic field ( $B_0$ ) of a few T. However, the ensemble dephasing time  $T_2^* \sim$  few nanoseconds. This can be improved by spin-echo techniques and a  $T_2$  time of  $\sim 3$   $\mu$ s has been

TABLE I. Required measurement time  $\tau_{\text{meas}}$  assuming  $\gamma = \gamma_1 + \gamma_2 = 1$  meV,  $V_{ex} = 0.2$   $\mu$ eV,  $P_e^{\text{sn}} = 0.04\%$ ,  $P_e^{\text{dark}} \sim N\Gamma\tau_{\text{meas}}$ ,  $P_e^{\text{rad}} \sim N\tau_{\text{meas}}/\tau_0$  ( $\tau_0 \sim 100$  ms), and  $P_e^{\text{total}} = P_e^{\text{sn}} + P_e^{\text{dark}} + P_e^{\text{rad}}$ . All  $P_e$ 's are listed in percent and  $\tau_{\text{meas}}$  is listed in nanoseconds.

	$\tau_{\text{meas}}$	$P_e^{\text{rad}}$	$P_e^{\text{dark}}$	$P_e^{\text{total}}$
Response of two-sided cavity				
Phase ( $V_s = 0$ )	64	0.028	0.0028	0.071
Intensity ( $V_s = 0$ )	28	0.01	0.001	0.05
Phase ( $V_s = 0.15$ meV)	72	0.04	0.003	0.08
Intensity ( $V_s = 0.15$ meV)	17	0.009	0.0007	0.05
Response of single-sided cavity				
Phase ( $V_s = 0$ )	8	0.005	0.05	0.095
Intensity ( $V_s = 0$ )	—	—	—	—
Phase ( $V_s = 0.15$ meV)	12	0.006	0.07	0.1
Intensity ( $V_s = 0.15$ meV)	28	0.01	0.17	0.2

achieved [25]. Thus, a measurement time  $\tau_{\text{meas}} \sim 10$  ns means that  $\sim 300$  QND readout operations can be performed before the qubit decoheres.

In conclusion, we have predicted that it is possible to perform a single-shot QND readout of the spin state of a QD electron by measuring the phase or the intensity response of a linearly polarized probe laser reflected from a cavity in which a QD is embedded close to a QW.

## ACKNOWLEDGMENTS

This work has been supported by the Japan Society for the Promotion of Science (JSPS) through its ‘‘Funding Program for World-Leading Innovative R&D on Science and Technology (FIRST Program)’’ and NICT. We thank Professor C. Piermarocchi, Dr. S. Höfling, Dr. C. Schneider, Professor D. Miller, Professor W. Harrison, Dr. M. Fraser, and Dr. T. Byrnes for insightful discussions.

- 
- [1] D. P. DiVincenzo, *Fortsch. Phys.* **48**, 771 (2000).
  - [2] N. C. Jones, R. Van Meter, A. G. Fowler, P. L. McMahon, J. Kim, T. D. Ladd, and Y. Yamamoto, *Phys. Rev. X* **2**, 031007 (2012).
  - [3] M. Atatüre, J. Dreiser, A. Badolato, and A. Imamoglu, *Nat. Phys.* **3**, 101 (2007).
  - [4] J. Berezovsky, M. H. Mikkelsen, O. Gywat, N. G. Stoltz, L. A. Coldren, and D. D. Awschalom, *Science* **314**, 1916 (2006).
  - [5] A. N. Vamivakas, C-Y. Lu, C. Matthiesen, Y. Zhao, S. Fält S, A. Badolato A, and M. Atatüre, *Nature (London)* **467**, 297 (2010).
  - [6] A. Delteil, W. B. Gao, P. Fallahi, J. Miguel-Sanchez, and A. Imamoglu, *Phys. Rev. Lett.* **112**, 116802 (2014).
  - [7] See Supplemental Material at <http://link.aps.org/supplemental/10.1103/PhysRevB.90.155421> for detailed derivation of exchange energy, phase and intensity response curves, error rates, justification of negligible polariton interparticle scattering and exciting the single polariton mode.
  - [8] C. Weisbuch, M. Nishioka, A. Ishikawa, and Y. Arakawa, *Phys. Rev. Lett.* **69**, 3314 (1992).
  - [9] H. Deng, G. Weihs, D. W. Snoke, J. Bloch, and Y. Yamamoto, *Proc. Natl. Acad. Sci. USA* **100**, 15318 (2003).
  - [10] M. I. Dyakonov, *Spin Physics in Semiconductors*, Springer Series in Solid-State Sciences (Springer-Verlag, Berlin/Heidelberg, 2008).
  - [11] I. A. Shelykh, A. V. Kavokin, and G. Malpuech, *Phys. Status Solidi B* **242**, 2271 (2005).
  - [12] C. Piermarocchi, P. Chen, L. J. Sham, and D. G. Steel, *Phys. Rev. Lett.* **89**, 167402 (2002).
  - [13] G. F. Quinteiro, J. Fernandez-Rossier, and C. Piermarocchi, *Phys. Rev. Lett.* **97**, 097401 (2006).
  - [14] S. Puri, N. Y. Kim, and Y. Yamamoto, *Phys. Rev. B* **85**, 241403(R) (2012).
  - [15] B. Urbaszek, R. J. Warburton, K. Karrai, B. D. Gerardot, P. M. Petroff, and J. M. Garcia, *Phys. Rev. Lett.* **90**, 247403 (2003).
  - [16] G. Björk, H. Heitmann, and Y. Yamamoto, *Phys. Rev. A* **47**, 4451 (1993).
  - [17] G. Björk, S. Pau, J. Jacobson, and Y. Yamamoto, *Phys. Rev. B* **50**, 17336 (1994).
  - [18] V. Savona, L. C. Andreani, P. Schwendimann, and A. Quattropani, *Solid. State Commun.* **93**, 733 (1995).
  - [19] K. Ujihara, *Jpn. J. Appl. Phys.* **33**, 1059 (1994).
  - [20] M. Osuge and K. Ujihara, *J. Appl. Phys.* **76**, 2588 (1994).
  - [21] G. Roumpos, W. H. Nitsche, S. Höfling, A. Forchel, and Y. Yamamoto, *Phys. Rev. Lett.* **104**, 126403 (2010).
  - [22] L. Klotzowski, M. D. Martín, A. Amo, L. Viña, I. A. Shelykh, M. M. Glazov, G. Malpuech, A. V. Kavokin, and R. André, *Solid. State Commun.* **139**, 511 (2006).
  - [23] G. Roumpos, C. W. Lai, T. C. H. Liew, Y. G. Rubo, A. V. Kavokin, and Y. Yamamoto, *Phys. Rev. B* **79**, 195310 (2009).
  - [24] A. Rahimi-Iman, C. Schneider, J. Fischer, S. Holzinger, M. Amthor, S. Höfling, S. Reitzenstein, L. Worschech, M. Kamp, and A. Forchel, *Phys. Rev. B* **84**, 165325 (2011).
  - [25] D. Press, K. De. Greve, P. L. McMahon, T. D. Ladd, B. Friess, C. Schneider, M. Kamp, S. Höfling, A. Forchel, and Y. Yamamoto, *Nat. Photon.* **4**, 367 (2010).